- Predicting re-emergence times of dengue epidemics at low reproductive
- 2 numbers: DENV1 in Rio de Janeiro, 1986-1990.
- 3 Rahul Subramanian, Victoria Romeo-Aznar, Edward Ionides, Claudia T. Codeço, and
- 4 Mercedes Pascual

5 Abstract:

Predicting arbovirus re-emergence remains challenging in regions with limited offseason transmission and intermittent epidemics. Current mathematical models treat the 8 depletion and replenishment of susceptible (non-immune) hosts as the principal drivers of re-emergence, based on established understanding of highly transmissible childhood diseases with frequent epidemics. We extend an analytical approach to determine the 10 number of 'skip' years preceding re-emergence for diseases with continuous seasonal 11 transmission, population growth and under-reporting. Re-emergence times are shown 12 to be highly sensitive to small changes in low R_0 (secondary cases produced from a 13 14 primary infection in a fully susceptible population). We then fit a stochastic SIR (Susceptible-Infected-Recovered) model to observed case data for the emergence of 15 dengue serotype DENV1 in Rio de Janeiro. This aggregated city-level model 16 17 substantially over-estimates observed re-emergence times either in terms of skips or outbreak probability under forward simulation. The inability of susceptible depletion and 18 19 replenishment to explain re-emergence under 'well-mixed' conditions at a city-wide 20 scale demonstrates a key limitation of SIR aggregated models including those applied to other arboviruses. The predictive uncertainty and high skip sensitivity to 21 epidemiological parameters suggest a need to investigate the relevant spatial scales of 22 susceptible depletion and the scaling of microscale transmission dynamics to formulate 23 24 simpler models that apply at coarse resolutions.

25 Introduction:

26 Epidemics of arboviruses such as dengue (1), Zika (2, 3), and chikungunya (4) 27 result in substantial global morbidity. Over the past decade, invasions of several 28 arboviruses have triggered large outbreaks in the Western Hemisphere. In Brazil, these invasions include dengue serotype DENV4 in 2012 (5) as well as Zika (2, 6) and 29 30 chikungunya (7) between 2014-2016. Predicting and understanding the re-emergence 31 of arboviruses after these invasions has important consequences for epidemic preparedness, particularly in regions where climate factors limit mosquito transmission 32 in the off-season. These regions typically exhibit highly intermittent seasonal 33 34 epidemics, lasting one to three years with long periods of no, or low, reported cases in 35 between, and low mean reproductive numbers (the number of secondary cases arising from each primary case in a completely susceptible population, R_0) (5, 8-10). Several 36 37 proposed explanations include the depletion of susceptible individuals following initial 38 epidemics (11) and the time required for their replenishment via population growth (12), inter-annual variation in climate (13-17), and antigenic interactions between strains of 39 40 different serotypes (18-21). These temporal patterns contrast with the recurrent seasonal outbreaks observed in childhood diseases with high reproductive numbers, 41 42 whose extensive study has provided the basis for our theoretical understanding of SIR 43 (Susceptible-Infected-Recovered) dynamics in infections that confer lifelong or lasting immune protection (22-29). 44 45 Statistical models of dengue transmission that take into account climate 46

Statistical models of dengue transmission that take into account climate

dependencies can be used to make short-term re-emergence forecasts on the order of

4 months (30) or 16 weeks (15). Many epidemiological models that predict the re
emergence of arboviruses such as Zika (11, 31) on longer time-scales of a year (11) or

49 several decades (31) rely however on compartmental formulations such as SIR-type 50 approaches (11) or Ross-McDonald equations that explicitly incorporate vector transmission (31). Both formulations assume transmission between any two individuals 51 in the population ('well-mixed' conditions), typically at aggregated spatial scales. These 52 53 process-based formulations, for example those recently applied to Zika, represent the acquisition of immunity in the population and its loss via demographic growth and 54 turnover. These models do take into account seasonality of transmission and spatial 55 56 heterogeneity in the intensity of transmission due to climate at coarse resolutions (at large city, state, or country-level scales). Nevertheless, the replenishment of a well-57 mixed susceptible population is frequently assumed to be the principal driver 58 59 determining when the disease will re-emerge given a particular seasonal pattern for R_0 at a particular location(31). Stochasticity can also play an important role in long-term 60 61 models of re-emergence (31). Variation in reporting rates of arboviruses between locations (32) can add further complexity. 62

63 Although childhood diseases with high reproductive numbers display different dynamics from emergent arboviruses (22-26), their compartmental models share a 64 65 basic SIR structure given the acquisition of long-term immunity after infection. The resulting depletion and replenishment of the susceptible population is known to clearly 66 drive inter-annual variability and re-emergence in the former (25, 27, 28). In particular, 67 68 recent theory (29) has derived analytical expressions for the number of "skip" years for a measles-like disease in the pre-vaccine era, where "skips" are defined as seasons 69 when transmission occurs but does not cause susceptible depletion. In other words, 70 although the number of infections increases in such seasons, it is not large enough to 72 offset the growth in the susceptible population due to demography. The resulting expressions specifically provide a threshold condition for the number of skips expected 73

following an initial invasion as a function of R_0 . Their derivation did not include underreporting and assumed a closed-population SIR model with 'school-term' seasonality, alternating two different rates for low and high transmission.

77 We examine in this work whether replenishment of susceptible individuals under 78 the typical 'well-mixed' assumption explains dengue (DENV1) re-emergence at the 79 whole-city aggregated level. We specifically address the uncertainty inherent in such predictions at the low reproductive numbers characteristic of arboviruses, not previously 80 81 considered in applications of the analytical approach. To this end, we first extend the 82 threshold derivation to take into account population growth, continuous (sinusoidal) seasonality, and under-reporting of cases. We then fit a stochastic SIR model to 83 observed monthly dengue case counts from the DENV1 invasion in Rio de Janeiro, 84 85 Brazil from 1986-1988 (8, 10, 33) and numerically predict expected times to re-86 emergence. We describe high uncertainty in re-emergence times for these seasonal, low transmission regions, and show the insufficiency of susceptible replenishment in a 87 simple SIR model to explain the short periods observed in DENV1 re-emergence. We 88 89 discuss possible explanations and the need for model formulations that would scale to 90 coarse spatial resolutions.

91

92 Results:

We start with the analytical approach for a seasonally forced SIR system with intermittent outbreaks and population turnover, to consider general features of reemergence at low R₀. In such a system, the onset of the off-season can bring an end to an initial outbreak, and the replenishment of susceptible individuals due to births and population turnover can be a major determinant of recurrence times. Let S represent

98 the number of susceptible individuals in a population and s₀, the fraction of the popula-99 tion still susceptible at the end of an initial epidemic, t₀, when a prediction for the time 100 to the next outbreak will be made. If there are enough susceptible individuals left in the 101 population (i.e. if s_0 is large), another outbreak will occur in the following year once the 102 on-season resumes. However, if the initial outbreak was very large, s₀ may be too small, and the outbreak may "skip" one or more years. A skip year is defined as a year in 103 104 which the susceptible population does not decrease, whether or not infections increase. 105 The smaller the fraction of the susceptible population at the time of prediction (s₀), the 106 longer it will take for the susceptible population to replenish, and the larger the number 107 of skips that will occur. Previous theory(29) allows prediction of the number of skips that will occur given s₀. Specifically, it demonstrated that s₀ must fall below some threshold s_c (k) for k skips to occur. An analytical expression was provided for $s_c(k)$ in 109 110 terms of the reproductive number and population turnover rate for a closed-population SIR model with school-term seasonality (29). The derivation of the threshold presented 111 in (29) requires the assumption that the transmission rate or reproductive number of the 112 113 disease is high and that the fraction of the population susceptible at the time of prediction (s_0) is small. 114

We extend this approach to take into account population growth and sinusoidal seasonality (which describes the transmission rate of dengue more accurately than a discrete high-low representation). Our derivation does not require assuming that the transmission rate or reproductive number are high or that the fraction of the population susceptible at the time of prediction is small. We follow the criteria developed in (29) (see details in (34)), which essentially consider the sign of the logarithm of the ratio between the respective number of infections at two times, t_0 and $t_n > t_0$. A positive value indicates that an outbreak will still occur at t_0 ; conversely a negative value indicates no

115

116

117

118

119

120

121

outbreak at that time. By setting the logarithm of this ratio to zero, the threshold s_c is obtained (See Section 1 of the Supporting Information for details).

The resulting expression for $s_c(n)$, the critical fraction of susceptible individuals required at the time of prediction for n or more skip seasons to occur, is

s_c(n) =
$$1 + \frac{\pi(2n+1)(1-\frac{1}{R_0})-2\delta}{\omega f(\omega,\delta,r,n)}$$
 (1)

where $f(\omega,\delta,r,n) = (1+e^{-r\frac{\pi}{\omega}(2n+1)})\omega\,\delta/(\omega^2+r^2) - (1-e^{-r\frac{\pi}{\omega}(2n+1)})/r$, R_0 is the annual mean of the reproductive number, δ , the amplitude of seasonal transmission (as infectious contacts per person per day), ω , the transmission frequency (in days⁻¹) and r , the population growth rate (also in days⁻¹). The full expression for the seasonal transmission rate is given by $\beta(t) = \beta_0(1+\delta sin(\omega t+\phi))$, where ϕ corresponds to the phase (in radians) and β_0 , to the mean seasonal transmission rate (infectious contacts per person per day). The quantity β_0 is related to the annual mean reproductive number R_0 via the expression $R_0 = \beta_0/\gamma$, where γ is the recovery rate (in days⁻¹).

Figure 1 illustrates the implications of this formula. As before, t_0 corresponds to the time of prediction, in practice usually after a large initial epidemic or invasion. Likewise, s_0 represents the fraction of the population susceptible at the time of prediction.

For n skips to occur, the fraction of the population susceptible at the time of prediction (s_0) must fall below the susceptibility threshold $s_c(n)$. Figure 1A shows that the larger the number of skips n one is considering, the smaller the threshold $s_c(n)$ that s_0

(s₀), the longer it will take for the susceptible population to replenish, and the larger the

number of skips that will occur. In practice, as we will illustrate below, values of s₀ can

be computed from surveillance data provided one has an estimate of the reporting rate.

140

141

142

143

144

must fall below for at least n skips to occur. Let n_c denote the critical skip number corresponding to the number of skips expected at the time of prediction (t_0). We use the fraction of the population susceptible at the time of prediction (s_0) and identify the maximum value of n for which s_0 is smaller than $s_c(n)$. In the example shown in Fig. 1A, this fraction $s_0 = 0.7$ is smaller than $s_c(n = 6)$ and bigger than $s_c(n = 7)$, which means $n_c = 6$. We therefore expect six years of skips followed by re-emergence in the seventh year. Formally, for a given value of s_0 at the end of the transmission season, we define the critical skip number n_c as the value of n for which $s_c(n_c) > s_0 > s_c(n_c + 1)$.



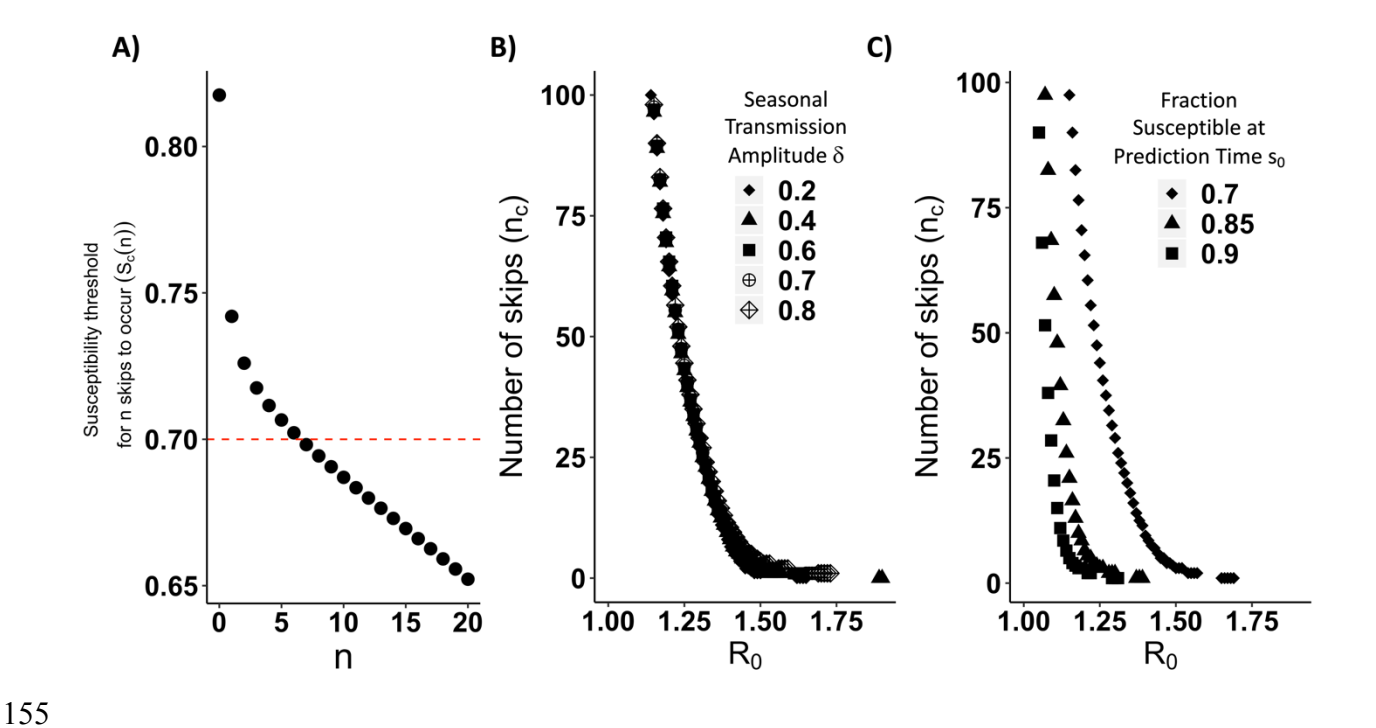


Fig 1. A) Graphical illustration of how the expected number of skips (n_c) is calculated. The black dots represent the threshold fraction of the population susceptible at the time of prediction required for n skips to occur $(s_c(n))$. The plot shows $(s_c(n))$ as a function of n (the number of skips) obtained from Equation 1 with seasonality amplitude δ =0.2 (contacts per person per day) and reproductive number R_0 =1.4. In this example, the red line represents the fraction of the population susceptible at the time of prediction (s_0) . If s_0 is smaller than $s_c(n)$, at least n skips will occur. To find the expected number of skips (n_c) , we identify the largest number of skips n such that s_0 is smaller than the susceptibility threshold required for those skips $s_c(n)$. In this example, the red line intersects the $s_c(n)$ curve between $s_c(n=6)$ and $s_c(n=7)$.

Therefore, a critical skip number of n_c =6 is obtained. **B) and C) The critical skip value** n_c as a function of R_0 for (B) different values of the amplitude of seasonal transmission δ with s_0 =0.7 and (C) different values of the fraction of the population susceptible at the time of prediction (s_0) with δ =0.70. In all three panels, the frequency of transmission ω , the population turnover rate μ , and population growth rate r are fixed at respective values $\omega = (2\pi/365)$ day⁻¹ corresponding to an annual periodicity, μ = 1/ (74.46*365)) day⁻¹ corresponding to an average lifespan of ~75 years, and r=1.55 μ day⁻¹ consistent with the growth of the city of Rio de Janeiro. These values were chosen for the purpose of illustration, based on the inverse of the average life expectancy in Brazil in 2012 according to the 2010 census (35), and the interpolation of population estimates for the resident population of the municipality of Rio de Janeiro from the 1991 (36) and 2000 (37) censuses assuming exponential growth.

178

179 With this general approach at hand, we explored the effects of the reproductive number R_0 , amplitude of seasonal transmission δ and fraction of the population 180 susceptible at time of prediction s_0 on the critical number of skips n_c (Figure 1 Panels B and C). Consideration of both the variation of the reproductive number R_0 and fraction of the population susceptible at time of prediction s_0 is relevant here. Different 183 combinations of transmission rate (β_0) and duration of the infection (1/ γ) can yield the same R_0 but different fractions of the population susceptible at the time of prediction (Supplemental Figure S16). Importantly, Fig. 1 panels B and C show that the time to reemergence is very sensitive to R_0 . A singularity is observed as R_0 approaches 1 where the expected number of skips goes to infinity. The approach to that singularity can be very steep, meaning that small changes in R_0 can result in large increases in the expected re-emergence time. The obtained values of n_c are not as sensitive to the 190 amplitude of seasonal transmission (Fig. 1 Panel B) but are sensitive to the fraction of 191 the population susceptible at the time of prediction (Fig. 1 Panel C). The shift of the curve in Fig 1 Panel C for small values of the fraction of the population susceptible at time of prediction s_0 means that, for a given R_0 , more time is required to replenish the susceptible population and therefore to observe a re-emergence.

196 We next apply this approach to the surveillance data from the 1986 invasion of 197 DENV1 in Rio de Janeiro (Figure 2). The initial DENV1 invasion in Rio de Janeiro is an 198 ideal initial test case for this technique given the lack of widespread prior immunity from 199 to prior dengue epidemics, vaccination campaigns, cross-immunity from other disease 200 outbreaks. Specifically, the 1986 invasion occurred prior to the development of dengue vaccines. The outbreak was the first dengue invasion in the area since the initial eradi-202 cation of the Aedes aegypti mosquito in Brazil in the 1950s (38-41) following a sus-203 tained intervention program that began in the 1930s and 1940s in Rio de Janeiro and other cities (39). Cross-immunity from yellow fever vaccination appears to be very lim-204 205 ited (42). Given the young age distribution of the population in 1986 (43), most individuals were not alive during the period when mass yellow fever vaccination or prior dengue epidemics occurred. 207

201

208 We let our time of prediction t_0 be equal to September 1, 1987, corresponding to 209 the end of the initial DENV1 invasion (see panel A of Figure 2). In panel B of Figure 2, we evaluate the number of expected skips expected in Rio de Janeiro, n_c , on the basis of a range of R_0 values from 1.18 to 2.02 from the literature (44, 45). The critical 211 susceptibility threshold for n skips to occur ($s_c(n)$) is calculated using Equation 1 with an 213 annual seasonality, a population growth rate interpolated from the census (see Materials and Methods section), and δ =0.7 (44). The fraction of the population susceptible at the 214 time of the prediction (s_0) is estimated as the difference between the total population N_0 216 (total population N at (t₀=Sep. 1987)) and the total number of people infected between the start of the invasion and the time of prediction (September 1, 1987). The total number of infected people during the outbreak is computed by summing the ratio 218 219 between the observed monthly cases and the reporting rate for DENV1 in the city. 220 Literature estimates from serology during the DENV1 invasion in Rio de Janeiro indicate

a reporting rate of around 3% (33) which we use and fix for this analysis. For comparison purposes, we also include the number of skips expected under a higher reporting rate of 10%. These curves show that the expected re-emergence could be very sensitive to small variation in R_0 and ρ , two quantities that are difficult to estimate with precision in the absence of serology. In particular, assuming a reporting rate of 3%, a reproductive number of 1.2 with 20% uncertainty can yield large changes in the expected re-emergence time. We highlight the potential sensitivity of the expected number of skips to the reporting rate as well to illustrate the importance of uncertainty in this parameter in cities or epidemics where its value is unknown.

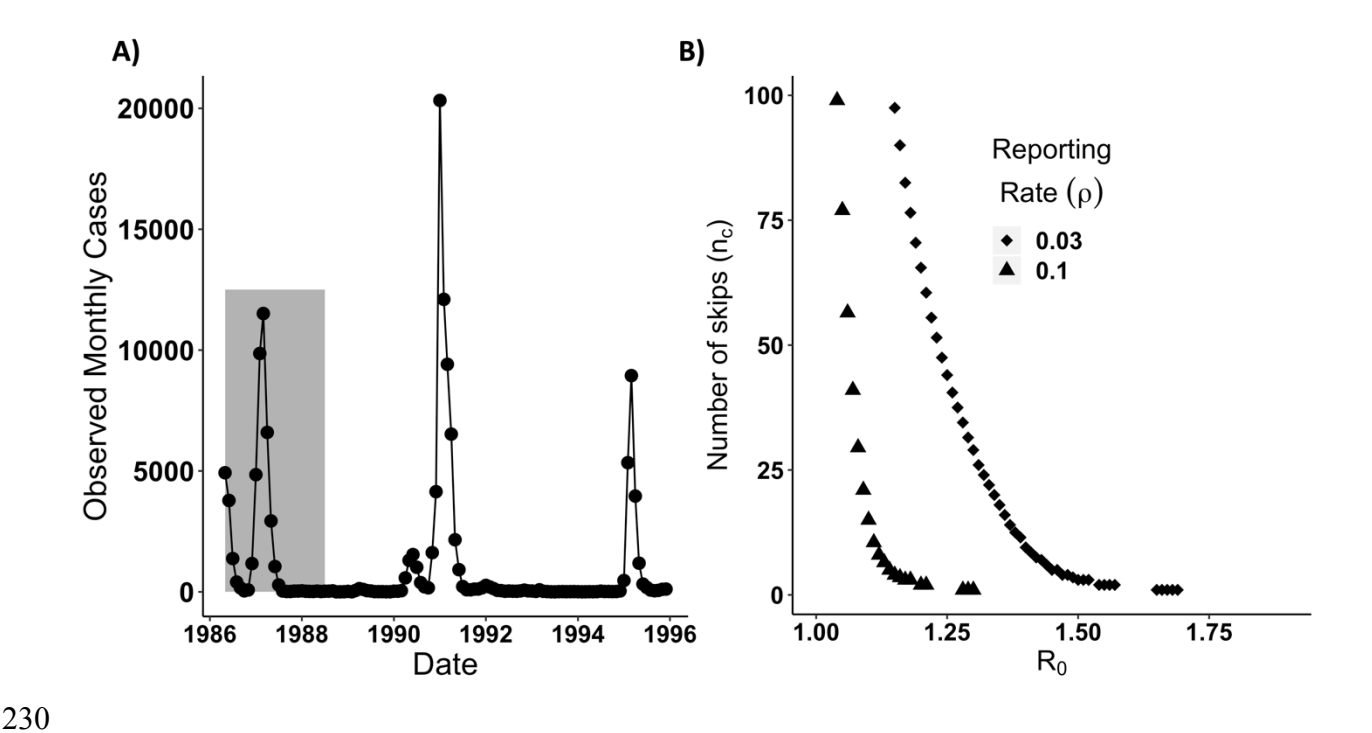


Fig 2. (A) Observed dengue case data. Monthly reported dengue cases in the city of Rio de Janeiro, Brazil from April 1986-1995. The grey shaded region denotes observations that were included in the fitting of the stochastic model from May 1, 1986 to July 1, 1988 inclusive. Serotype DENV1 re-emerged in 1990. DENV2 was first detected in the state of Rio de Janeiro in 1990 but did not become dominant until 1991 (8, 9). Both co-circulated afterwards. We focus on the invasion of DENV1 from 1986-1987 and its initial re-emergence in DENV1 in 1990 using a single serotype transmission model. This allows us to evaluate this transmission model in a region where only one serotype was circulating, where cross-immunity could not easily be invoked to explain the absence or reduction of dengue in a given year. (B)

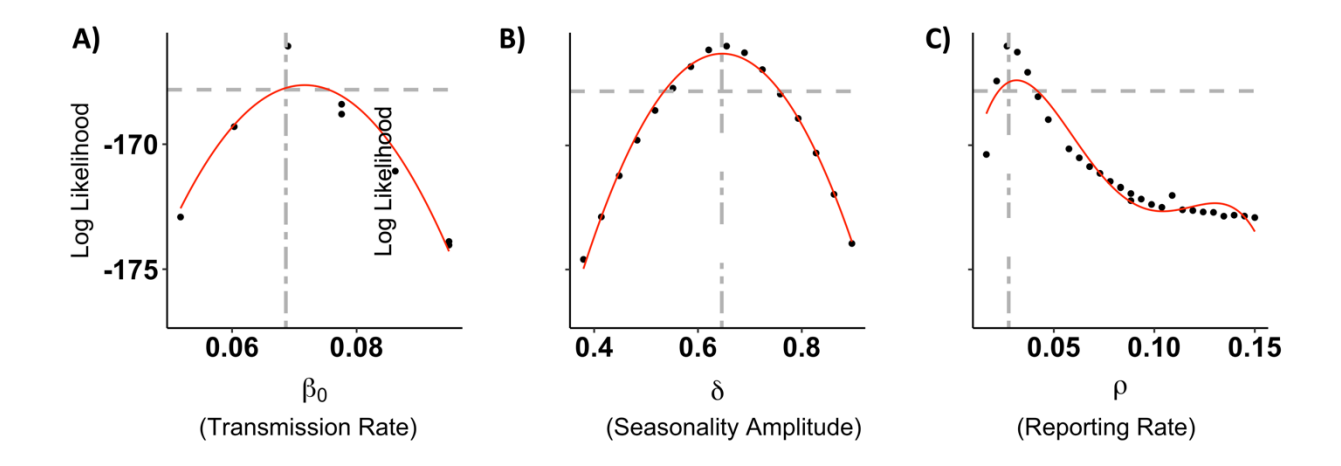
Deterministic critical number of DENV1 skips n_c for Rio de Janeiro from September 1988. Expected number of skips n_c with amplitude of seasonal transmission δ =0.7 and the fraction of the population susceptible after the first DENV1 invasion as of September 1, 1987 (s₀) calculated from the data (A). We use a reporting rate ρ of 3% when calculating s₀, consistent with serological estimates from the literature (33). For comparison purposes, we also include the expected number of skips n_c assuming a reporting rate of 10%.

249

248

Replenishment of Susceptible Individuals is Insufficient to Explain Re-Emergence

251 To obtain more precise bounds for the reporting rate and R_0 and to determine if the depletion and replenishment of susceptible individuals could explain the rapid re-253 emergence of dengue in Rio de Janeiro, we fit a stochastic aggregate SIR model to case data from the DENV1 invasion from 1986-1988. The stochastic SIR model assumes that the underlying deterministic transmission rate varies seasonally as a 255 sinusoidal function with annual mean β_0 , seasonal transmission amplitude δ , frequency 256 257 ω (equal to $2\pi/365$), and phase ϕ . The model takes into account demographic 258 stochasticity, environmental stochasticity in the transmission rate, and measurement 259 error due to under-reporting and variation in reporting of cases (See Materials and 260 Methods and the Supporting Information). Panels A,B, and C of Figure 3 show the 261 likelihood profile of the annual mean transmission rate, β_0 , the amplitude of seasonal 262 transmission δ , and the reporting rate ρ , respectively. In particular, our estimate of the reporting rate matches that from serology in the literature (Panel C). 263



264

265 Fig 3. A-C) Selected parameter profiles for the stochastic model. Profiles of the 266 mean annual transmission rate β_0 (A), seasonal transmission amplitude δ (B), and 267 reporting rate ρ (C). The red curve is a polynomial fit to the subset of the profile points 268 shown on the figure. The single dashed grey horizontal line represents the likelihood 269 value 2 log likelihood units below the maximum likelihood estimate. This line provides 270 an estimate of confidence intervals for the given parameter. The grey vertical line 271 denotes the parameter value of the maximum likelihood estimate. The maximum likelihood estimate for the reporting rate in panel C is very close to the literature value obtained from serology (approximately 3 percent). (33).

274

275

278

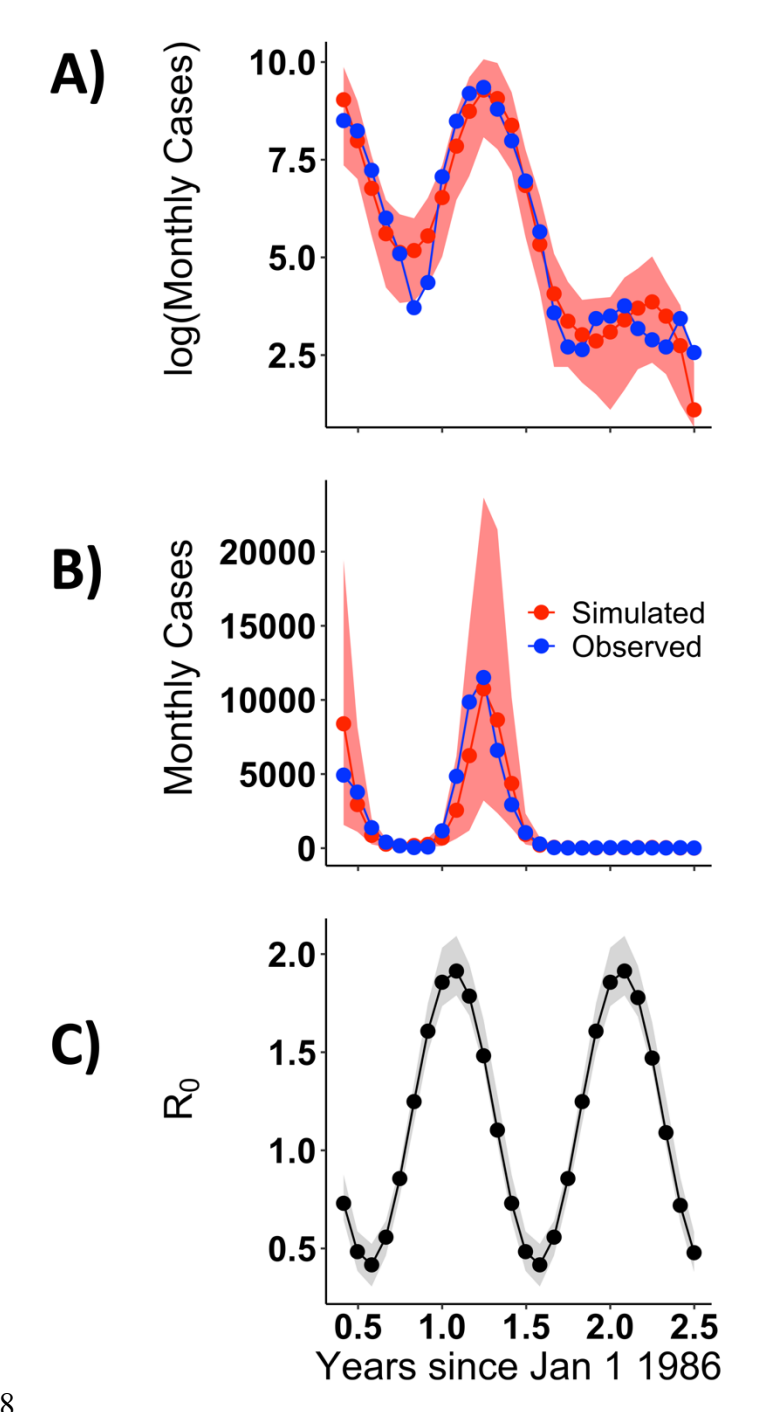
280

281

273

Overall, the model is able to capture key dynamics of the DENV1 invasion including the two peaks of incidence in 1986 and 1987 and the subsequent reduction of transmission in 1988. This is shown by comparing the trajectories for an ensemble of simulations with the fitted model to the observed values of cases (Fig. 4). Estimated values for the transmission rate indicate a low value for R_0 (Figure 4 Panel C). Both of these conclusions generally hold even if one takes into account uncertainty in parameter estimates by examining all parameter combinations with log likelihoods within 2 log likelihood units of the maximum likelihood estimate (the grey region in Figure 4 Panel C as well as Supplemental Figure S1), although some parameter

combinations (not the maximum likelihood estimate) have substantial process noise(Supplemental Figure S1).



290 Fig 4. A-B) Comparison of simulated values with the fitted model and observed 291 data on a log (A) and regular (B) scale. Observed monthly cases from April 1986 to 292 June 1988 are shown in blue. Median values from 100 simulations with the maximum 293 likelihood parameter combination are shown in red. The shaded red region denotes the 294 2.5% and 97.5%th quantile boundaries from those simulations. C) Estimates for $R_0(t)$. 295 The black line denotes the trajectory of $R_0(t)$ for the maximum likelihood estimate. The 296 shaded grey region represents the 2.5% and 97.5%th quantile boundaries for 297 trajectories from all parameter combinations within 2 log likelihood units of the maximum 298 likelihood estimate. Each parameter combination has only one seasonal trajectory for 299 $R_0(t)$ since $R_0(t)$ is a deterministic quantity. $R_0(t)$ for all parameter estimates ranges from 1.79-2.09 in the on season to 0.31-0.52 in the off-season. 300

301

302

303

305

307

We now apply the obtained parameter estimates from the fitted model to address the expected re-emergence time on the basis of, first, the analytical expression 304 for the skip calculation (Equation 1), and then the stochastic simulations of the fitted model. The parameter estimates used here are those for the reporting rate ρ , the reproductive number R_0 , and the amplitude of seasonal transmission δ from all combinations within 2 log likelihood units of the MLE. The expected number of skips following the DENV1 invasion in 1986-1988 is considerably higher than the observed 2 years. Depending on the parameter combination used, we obtain anywhere from 27 to 100 skips (Panel A of Figure 5). Even the fastest estimated return from the skip analysis (27 years) is much slower than the observed re-emergence time.

312 Forward simulation of the stochastic model likewise does not predict the rapid reemergence of DENV1 (Panel B of Figure 5). Under a pulse of 20 infected individuals 314 arriving per day, there was a low probability of re-emergence for parameter combinations with low process noise (Panel B of Figure 5). Only parameter combinations with high amounts of process noise (which have limited predictive value) 317 had a non-zero emergence probability. We consider alternate pulse rates in

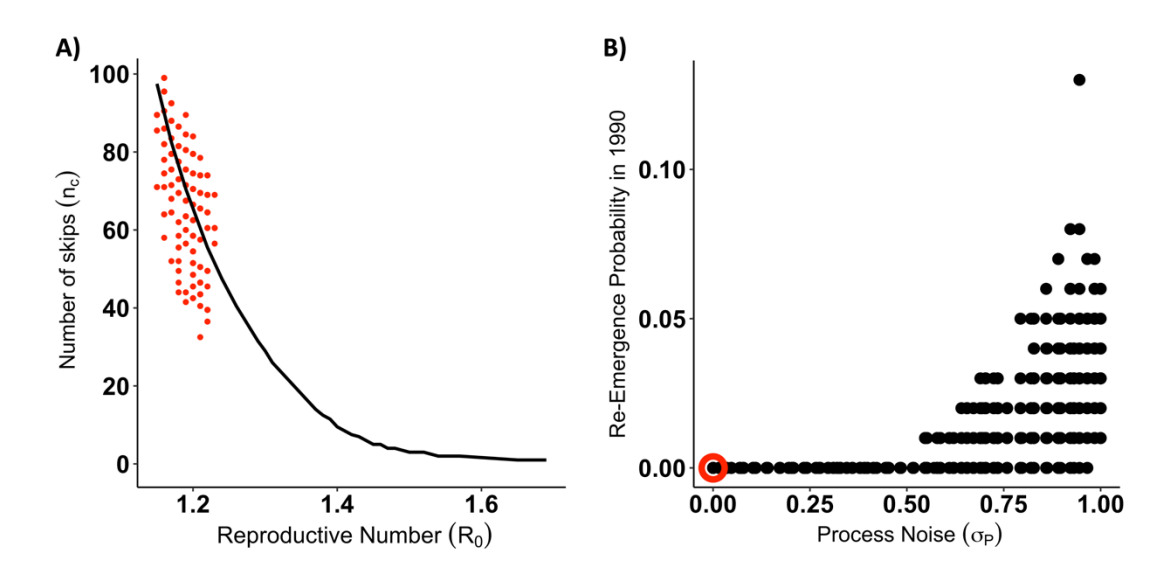
Supplemental Figure S14. Re-emergence probabilities under forward simulation of the stochastic model thus corroborated the deterministic skip findings. The depletion of susceptible individuals from 1986-1988 and their replenishment via population growth from 1989-1990 under an aggregate SIR model was unable to explain the rapid reemergence of DENV1 in 1990.



319

320

321



324

Fig 5. A) Expected number of skips (n_c) calculated using parameters obtained 326 from the fitted stochastic model. The open circles show the expected number of skips n_c from Equation 1 using parameters and the fraction of the population susceptible 327 328 after the initial DENV1 invasion (s₀) estimated from the fitted stochastic model. Each 329 circle corresponds to one parameter combination, and we included here all parameter combinations for the fitted model with a seasonal transmission amplitude (δ) of 0.7 (contacts per person per day) and a likelihood value within two log-likelihood units of the 332 maximum likelihood estimate (MLE). See Figure S15 for expected skips from parameter combinations with different values of δ , and Figure S10 for parameter 333 334 combinations from the profile of the recovery rate, γ . For comparison purposes, the black line shows the expected number of skips for the deterministic skip calculation from panel B of Figure 2 with the reporting rate ρ fixed at the literature value of 3%. **B)** Probability of epidemic in 1990 under forward stochastic simulation of fitted 338 model. The fitted stochastic model was simulated forward in time from 1986-1990 with population growth. A pulse of 20 infected individuals were assumed to arrive each day in January 1990. Each parameter combination within 2 log likelihood units of the maximum likelihood estimate was simulated 100 times. The re-emergence probability was calculated by determining the number of simulations in which the susceptible

- population decreased in 1990. The plot shows re-emergence probability as a function of
- the process noise intensity σ_P . Each point represents a single parameter combination.
- The maximum likelihood estimate parameter combination is circled in red.

Sensitivity Analysis:

To examine the robustness of our findings to adding an incubation period or altering the form of seasonality, we conducted a sensitivity analysis by considering both SIR and SEIR models with spline seasonality. The results are presented and discussed in the Supporting Information and show that our conclusions remain unchanged. (See the Supporting Information including Supplemental Figures S2-S7 and Supplemental Tables ST2 and ST3).

354 Comparison with Vector Model and literature R₀

The fitted stochastic SIR model uses a cosine function as a simplification to represent the seasonal forcing that would be created by climate variation (temperature (46)) via the changes in infected mosquitos. To evaluate whether this simplification is realistic, we take two approaches. The first one compares the mean seasonal R₀ resulting from our model to values of this reproductive number directly estimated from time series data in the literature for DENV1 and DENV4 in Rio de Janeiro from 2010-2016. There is a close match between these very different ways to estimate R₀, and in particular the shape of the seasonality produced by our model is realistic (Supplemental Figure S18).

The second approach considers a simple temperature-driven vector model. To this end, we initially show that the seasonal variation in temperature in Rio de Janeiro can be approximated via a cosine function (Panel A of Supplemental Figure S19 and use this approximation to drive a transmission rate that includes the vector explicitly.

To obtain an expression for the seasonal transmission rate we consider an ex-plicit mosquito model with compartments for infectious and susceptible mosquitoes in which a number of parameters depend on temperature (T) (see Section 4 of the Sup-porting Information). By assuming fast dynamics of the mosquito (so that levels of in-fection in the mosquito population quickly equilibrate to the dynamics of infection in the human population), we derive the following expression for the effective transmission rate in the mosquito-human model in terms of the biting rate a(T), probability of human infection given an infectious bite b(T), probability of mosquito infection given biting of an infectious human pMI(T), adult mosquito mortality rate μ_M , carrying capacity K of the mosquito population, human population size N, and mosquito demographic function g(T):

$$\beta_{eff} = \frac{a(T)^2 b(T) (pMI(T))}{\mu_M} \frac{K}{N} \left(1 - \frac{\mu_M}{g(T)} \right)$$
 (2)

The function g(T) is the product of the eggs laid per female mosquito per gonotrophic cycle, the mosquito egg-to-adult survival probability, and the mosquito egg-adult development rate divided by the adult mosquito mortality rate μ_M . The temperature-dependence of these components was borrowed from the literature (47, 48) (see Supporting Information Section 4 for details).

Under the fast dynamics assumption, this effective transmission rate β_{eff} is an implicit representation of the force of infection inflicted on humans by the vectors of the coupled human-vector model. When re-scaled between 0 and 1, β_{eff} corresponds closely with β_{MLE} , the transmission rate from the fitted stochastic SIR cosine model (Panel B of Supplemental Figure S19). This close correspondence indicates that the

390 SIR cosine model is able to capture the shape of the seasonality of DENV1 in Rio de 391 Janeiro.

392

394

396

398

399

401

402

403

404

405

406

407

408

409

410

411

412

413

393 Discussion

We developed two lines of evidence regarding the uncertainty and predictability of the time to re-emergence for diseases with low reproductive numbers on the basis of a seasonally forced SIR model under the 'well-mixed' assumption at aggregated, citywide, scales. We showed with an analytical approach that the time to re-emergence (expressed as the number of "skip" years) was highly sensitive to small changes in R_0 and the fraction of the population still susceptible s_0 at the time of prediction (e.g. at the end of the initial outbreak). This sensitivity applies to dengue in Rio de Janeiro where re-emergence times can vary on the order of decades based on literature parameters. This uncertainty contrasts with previous applications of this analytical approach to SIR dynamics in childhood diseases such as measles with much higher R_0 values where accurate predictions of much shorter skip times have been made (29). We also showed with a stochastic SIR model with seasonal transmission fit to DENV1 observed case data for Rio de Janeiro from 1986-1988 that susceptible depletion and replenishment are insufficient to explain dengue re-emergence. The fitted model failed to predict by far the re-emergence of DENV1 in 1990 in terms of either the number of skips expected or the outbreak probability under forward simulation.

Transmission parameters like R_0 are generally defined with respect to a particular model. Given that we aggregated cases at the city level and used a short time series, care should be taken in interpreting parameter values. Nevertheless, fitted transmission parameters correspond well with literature values and exhibit well-defined confidence

intervals. Estimates of the reporting rate in particular closely match the 3% value (8) 415 obtained via a serological study conducted during the 1986 invasion (8, 33). Reporting rates during the onset of an epidemic may be much lower in regions that have not 416 recently experienced transmission (33, 49) than in those with re-occurring outbreaks 417 418 and an established surveillance network. This may explain why serological studies of 419 the 1986 invasion (8, 33) and our results, estimate a lower reporting rate for dengue 420 than studies conducted in later years in Brazil (50). Even though different combinations 421 of the transmission rate and duration of infection can yield the same reproductive number, the parameter estimates that compose R₀ across all models considered in the 422 423 sensitivity analysis (which take into account those different combinations) are relatively well-defined. These values are also consistent with the effective reproductive number 425 estimated for local dengue epidemics from 2012-2016 (44) and 1996-2014 (45) taking 426 into account differences in serotype circulation and population size during those 427 periods.

More complex model structures are possible and often used for arboviruses that include an explicit representation of the vector. We expect our results to hold as this vector component should largely affect the phase and shape of seasonality in the transmission between human hosts, which we have modeled phenomenologically as a cosine wave. With two typical successive epidemic years from an emergent virus, parameter inference from such short observation period is unlikely to justify a more complex model. Nevertheless, to examine transmission seasonality further, we compared the seasonal R_0 resulting from the fitted model to the seasonal R_0 directly estimated from time series of cases in the literature (44). We also considered the transmission rate experienced by humans in a simple vector-human model forced by the typical seasonality of temperature in Rio de Janeiro. The shape and timing of the

428

429

431

433

434

435

436

437

vector-human model's transmission rate was comparable to that of the cosine transmission rate we employed. More complex models that do not assume fast dynamics of infection in the vector relative to epidemic spread would likely exhibit a difference relative to our transmission rate, especially a delayed phase, whose consequences should be examined in future work. We posit that this difference would not influence our results on the predictability and uncertainty of re-emergence, since the values of other parameters (such as the length of infection in humans) can compensate 446 for it.

439

440

441

442

443

444

447

448

449

450

451

452

454

456

457

458

459

460

461

462

Factors that could explain the observed rapid re-emergence include inter-annual climate anomalies, antigenic evolution, or micro-scale spatial heterogeneity in transmission intensity and associated susceptible depletion. Larvae washout following flooding coupled with temperature-driven seasonality in transmission could have temporarily halted the invasion in 1988 and delayed the epidemic in 1989. Widespread flooding was reported in February 1988 (51). Large amounts of rainfall washed away mosquito larvae in lab and field studies (52). High rainfall negatively affected dengue transmission in Singapore (53, 54) and India (55). The impact could be compounded in Rio de Janeiro if the high rainfall occurs during the transmission season. If the larvae population has not fully recovered before the start of the off-season, the impact of the rainfall anomaly could extend to the subsequent season.

The large amount of process noise observed in the aggregate model would be consistent with this effect, given that the process noise parameter σ_P represents random variation in the transmission rate due to environmental factors. However, the model's inherent structure limits its ability to take into account flooding events via σ_P , since the magnitude of the process noise does not change between years. Incorporating an interannual climate driver could provide more accurate re-emergence predictions. The
 response to rainfall would be nonlinear: positive at low to moderate levels and negative
 at higher ones.

466 Intra-serotype antigenic evolution from 1986-1990 could also facilitate faster re-467 emergence. Many models focus on inter-serotype variation and assume long-lasting 468 homosubtypic immunity (18, 19, 21). However, the antigenic variation within and across dengue serotypes is comparable (56), and antigenic differences between strains of the 469 same serotype influence overall dengue evolution(57). Sequences associated with 470 471 case data were unavailable, making direct analysis challenging. We cannot rule out the possibility that genetic differences between the circulating strains enabled re-infection. A 472 473 future SIRS-type model (Susceptible-Infected-Recovered-Susceptible) could 474 incorporate this intra-serotype antigenic evolution.

475 Micro-scale spatial heterogeneity in transmission intensity and the effects of 476 human movement between neighborhoods could also explain the rapid re-emergence. 477 Small-scale differences in socioeconomic status and population density between 478 neighborhoods in a large city can result in different relationships between mosquito and 479 human population sizes, resulting in widespread heterogeneity in R_0 across neighborhoods (58). Previous studies of mosquito trap data in the city have 480 demonstrated that neighborhoods with differing socioeconomic characteristics have 482 different vector population patterns (46). In fact, schoolchildren from neighborhoods 483 with divergent socioeconomic characteristics had varying levels of seroconversion 484 during the 1986 invasion (33). Human movement between neighborhoods may also 485 influence transmission within (59) and between (60) those neighborhoods, potentially 486 resulting in non-uniform depletion of susceptible populations between highly connected

and isolated areas of a city. Whether arising through the effects of spatial heterogeneity in transmission or intra-city movement, non-uniform levels of herd immunity could enable faster re-emergence.

490 Our findings reveal the uncertainty of re-emergence predictions with the simplest 491 SIR models, those that would be most useful at times of emergent public health threats. 492 Consideration of the above factors in transmission models whose goal is to inform 493 public health over large regions, and to do so soon after, if not during, an emergent 494 outbreak, is clearly a challenge. For example, coarse resolutions are typically used 495 because of the scales at which the observed cases are reported, the scales at which the 496 climate covariates are available, and the difficulties inherent in incorporating microscale 497 variation including connectivity. Our results should motivate further research into the 498 central question of how we can scale microscale heterogeneity to formulate aggregated models that include it implicitly. It should also motivate the related further understanding 499 500 of how such microscale heterogeneity influences susceptible depletion and replenishment in particular case studies. From such efforts, we should be able to 502 evaluate whether the increasing availability of high-resolution data makes it feasible to 503 parameterize transmission models at higher resolutions, or to inform new model 504 formulations at coarser resolutions.

The inability of susceptible depletion and replenishment in a simple seasonal SIR formulation at a large, city-wide scale, to explain DENV1 re-emergence has potential implications for other arboviruses. Recent long-term Zika forecasts (31) assume that susceptible depletion and replenishment brought an end to the 2015-2017 epidemics and will determine when re-emergence occurs. DENV1 and Zika share the same vector and invaded a completely susceptible population (not accounting for pre-existing cross-

505

506

507

508

509

immunity from dengue). If factors absent from the basic model were key drivers of
DENV1 inter-annual variability, it would not be unreasonable to infer that similar types of
factors could have played a major role in the Zika dynamics observed from 2015-2017.
Zika re-emergence could similarly occur much earlier than expected.

With changing temperature patterns due to climate change, cities in Asia,

Europe, and the western hemisphere that currently do not have recurrent local

transmission may transition in the near future to the kinds of dynamics studied here. Our

results suggest that estimates should be interpreted in the context of this sensitivity to

small changes in the reporting rate and reproductive number. Factors like variation in

reporting rates, micro-scale transmission heterogeneity and inter-annual climate drivers

that are often ignored in long-term forecasts may thus become critical in determining re
emergence times. Overall, the large uncertainty in re-mergence times may be

unavoidable for these regions. Improved models are needed together with richer data

than currently used, to address the question of the relevant spatial scales of susceptible

depletion.

Materials and methods

The derivation of the expression for the number of skip years (Equation 1) is included in Section 1 of the Supporting Information. We fitted a stochastic version of the SIR model to observed monthly case counts in Rio de Janeiro from 1986-1988 to estimate parameters needed to apply this expression, and also to separately predict in parallel the time to re-emergence via numerical simulation. Expected re-emergence times were then compared for the two approaches.

534 Data Description

We used monthly dengue case estimates in the city of Rio de Janeiro, Brazil from 1986-1990. Cases were reported to the local public health surveillance system (9, 10). The case counts did not contain serotype information, but prior studies indicated that the dengue serotype DENV1 invaded the city of Rio de Janeiro in 1986 (10) and was the dominant serotype in circulation in the state of Rio de Janeiro from 1986-1990 (8) prior to the arrival of DENV2 in 1990. DENV2 did not become dominant until 1991 (9).

Basic Model Formulation

Because dengue infection confers full immunity to the same serotype, we
considered an SIR (Susceptible-Infected-Recovered) model. The deterministic model
for the number of individuals in the Susceptible (S), Infected (I), or Recovered (R) class
is given by the following system of ordinary differential equations:

$$\frac{dS}{dt} = rN - \lambda(t)S - \mu_H S$$
(3)
$$\frac{dI}{dt} = \lambda(t)S - \gamma I - \mu_H I$$
(4)
$$\frac{dR}{dt} = \gamma I - \mu_H R$$
(4)

 $\lambda(t) = \beta(t)(\frac{I}{N})$ (5)

547

550

551

552

553

554

555

556

557

558

560

561

562

563

565

566

567

568

569

570

$$\beta(t) = \beta_0 (1 + \delta \sin(\omega t + \phi))$$
(6)

Deaths occur at rate (μ_H) given by the inverse of the life expectancy of Brazil in 2012 (74.49 years(35)). All individuals are born susceptible. The term r represents population growth. The human population growth rate was estimated from census resident population estimates in 1991 (36) and 2000 (37) assuming exponential growth. This rate was used to interpolate the estimated population in 1986 (See Supporting Information Section 2.1.1 for details).

The per capita rate at which susceptible individuals become infected was given by the force of infection $\lambda(t)$ (Equation 5). Individuals recovered at per-capita rate γ whose inverse is the duration of infection. Estimates of the duration of infection in dengue vary. One analysis estimated that symptoms of dengue infection last 2-7 days following an incubation period of 4-10 days (61, 62). For our analysis, we fixed the recovery rate γ to be 1/17, assuming an exponentially distributed duration of infection with mean of 17 days encapsulating the maximum extent of the combined incubation and symptomatic period in humans. We take into account the possibility that duration of infection could vary by profiling over the duration of infection in the sensitivity analysis. The short duration of the available time series meant that fitting a formal vector model could prove difficult and could require additional assumptions in terms of which parameters could be fitted or fixed from existing formulations in the literature. We therefore used an SIR framework in which the infected stage served as a proxy for the exposed and infected human compartments in a vector model of dengue transmission, and we assumed infection levels in vector rapidly equilibrate with those in humans (as described later when we consider the vector explicitly (See Section 4 of the Supporting Information). A duration of infection was thus chosen that corresponds to the upper bound of the estimated pre-infectious period (4-10 days) and infectious period (2-7 days) in humans (61, 62). We profiled over the duration of infection in the sensitivity analysis to verify that this parameterization is reasonable.

This transmission rate $\beta(t)$ was represented as a cosine function with mean β_0 , (units of contacts per person per day) and seasonal oscillations of amplitude δ (same units as β_0) and frequency ω , which was assumed to be annual ($\omega = 2\pi/365$) days⁻¹. The annual mean R_0 was thus given by:

$$R_0 = \frac{\beta_0}{\gamma + \mu}$$
(8)

The observed dengue data in Rio de Janeiro consisted of monthly case counts. Serological studies of the DENV1 invasion in Rio de Janeiro also indicated substantial under-reporting (8, 33). Let C represent the true number of monthly cases that would be obtained by summing the number of individuals entering the infected class (I) over the course of a month. For the purposes of the skip analysis, we assume that a fixed fraction ρ of the true cases C are observed, where ρ is the reporting rate.

The stochastic model is an approximation of the deterministic one used for the skip analysis. For simplicity and given the short time interval, we assumed that there was no population growth over the two and half years of the DENV1 invasion ($r = \mu_H$) and that births and deaths occurred at rate $\mu_H = (1/(74.9*365))$, which is equal to the inverse of the average life expectancy in Brazil from the 2010 census (35). However, population growth is taken into account when simulating forward in time from the fitted

592 stochastic model. We also assumed that there were no recovered individuals at the start 593 of the epidemic, so all other individuals in the population not initially infected were susceptible. We considered time in units of days and used a time step Δt of 1 day. 594 595 The stochastic model is a discrete-time model with fixed time step Δt and a discrete state space (i.e. the number of people in each compartment S, I, R, and C, at any point 596 597 in time must be integers). The number of individuals who moved from one compartment to another over the course of each day was calculated via Euler simulation from the 598 deterministic equations (See Supporting Information). Demographic stochasticity was 600 then incorporated into the Euler approximations to obtain integer state variable values 601 after each time step. We specifically assumed that the number of individuals making 602 each state transition was drawn from a binomial distribution with exponentially decaying 603 probability (See Supporting Information). Environmental noise (variation in the transmission rate $\beta(t)$ due to random environmental variation) was captured via 604 multiplicative gamma white noise in the transmission rate as described by (63, 64). On 605 time step size Δ t, we multiplied the transmission rate by $\Delta\Gamma$ / Δ t, where $\Delta\Gamma$ / Δ t was drawn from a Gamma distribution with mean 1 and variance $\sigma_P^2 / \Delta t$. 607

The measurement model assumed that the observed number of monthly dengue cases (Y(t)) at time t were drawn from a negative binomial distribution with mean equal to the true number of monthly cases C multiplied by a reporting rate ρ , with dispersion parameter σ_M . More details of the measurement model can be found in Section 2.4 of the Supporting Information.

Fitting the stochastic model

608

609

611

We fitted the transmission parameters (β_0 and δ), reporting rate (ρ), process noise parameter ($\sigma_{\rm P}$), measurement noise parameter ($\sigma_{\rm M}$), and the number of infected individuals at the start of the outbreak in May 1986 (I_0). While the first cases of DENV1 were reported in April 1986, we started the model fitting in May 1986 to avoid complications from changes in the reporting rate as the surveillance system was established during the start of the DENV1 invasion. We used in an interpolated initial population size of 5,281,842 for Rio de Janeiro in May 1986. The model was fit using the mif2 method in the R-package pomp. The model fitting method is described further in the Supporting Information and in (65).

Calculating expected skips using parameter estimates from stochastic model

Following the completion of the Monte Carlo Profiles, a maximum likelihood estimate (MLE) parameter combination was obtained from the Monte Carlo Profiles of the fitted model by selecting the parameter combination with the highest likelihood across all profiles. The table of MLE parameter values is shown in Supplemental Table ST1. All sets of parameter combinations within 2 log-likelihood units of the maximum likelihood estimate (from all profiles) were used for the expected skip calculation. The reporting rate (ρ), β_0 , and δ value of each parameter combination within 2 log likelihood units of the maximum likelihood estimate were applied to a finer gridded version of the deterministic skip calculation described earlier. A distribution for the number of skips expected in Rio de Janeiro following the DENV1 invasion from 1986-1988 was obtained.

Stochastic Simulation

We then simulated re-emergence probabilities under the stochastic model. Each parameter combination within 2 log likelihood units of the MLE estimate from the

638 stochastic fit was simulated again without any immigration from 1986 until 1990 but with 639 population growth. During January 1990, "sparks" of infectious individuals were assumed to have arrived in the city at some fixed rate. There were low but non-zero 640 levels of DENV1 incidence from 1988-1989. We chose to wait until January 1990 before 641 642 introducing new DENV1 infections to be conservative, as this is when an uptick in 643 DENV1 incidence was first observed. Had we introduced sparks earlier in 1988-1989, we would likely have observed even earlier re-emergence times. We explored rates 644 from 5 to 100 infected individuals per day. This process was repeated 100 times, and the probability of an epidemic occurring in 1990 was calculated. An epidemic 646 occurrence in this situation was defined as a net decrease in the susceptible population 647 over the course of the year (after taking into account population growth), to best match 649 the definition of an epidemic used in the skip analysis.

Sensitivity Analysis

650

657

658

659

660

661

We assessed how parameter estimates of R_0 and ρ may depend on the model formulation by fitting several more complex SIR-type models to the same data using the fitting procedure described in the Methods section: an SIR Spline Model and SEIR Spline Model. As an additional sensitivity analysis, we profiled over the recovery rate for the SIR Cosine Model (Supplemental Figure S9). For details, see the Supporting Information.

Comparison with Vector Model and literature R₀

For a full description of the explicit coupled human-mosquito model with compartments for infectious and susceptible mosquitoes and comparison of transmission rates between this model and the simpler seasonally forced SIR, see the Supporting Information.

663 Author Contributions

- 664 RS, VRA, MP designed the experiments. RS and VRA conducted the experi-
- 665 ments. RS and EI developed the stochastic model fitting pipeline. CC provided
- 666 the data and expertise on dengue in Rio de Janeiro. RS, VRA, and MP drafted
- the manuscript. All authors contributed to the writing of the manuscript.

668

669 Acknowledgements

- The authors would like to thank Aaron King for his advice, and two referees
- 671 for their insightful comments. This work was completed with resources and
- 672 support provided by the University of Chicago's Research Computing Cen-
- 673 ter.

674

675 Data Accessibility

- 676 Data and code used to fit the stochastic model is accessible via a public
- 677 GitHub repository (https://github.com/pascualgroup/JRSI DENV1 skips Rio
- 678).

679

680 Ethics

- 681 This article does not present research with ethical considerations. The authors
- 682 declare that they have no competing interests.

683

684 Funding Statement

- RS was supported by a National Science Foundation Research Train-
- 686 eeship (# 1735359: NRT-INFEWS: Computational data science to advance
- 687 research at the energy environment nexus). MP and EI were supported by
- 688 a collaborative grant from the National Science Foundation's Division of
- 689 Mathematical Sciences and the National Institutes of Health (# 1761612:
- 690 Collaborative Research: Urban Vector-Borne Disease Transmission De-
- 691 mands Advances in Spatiotemporal Statistical Inference). VRA was jointly
- 692 supported by this grant and by the Mansueto Institute for Urban Innovation
- 693 through a Mansueto Institute Postdoctoral Fellowship.

694

- 695 The funders had no role in study design, data collection and analysis, deci-
- 696 sion to publish, or preparation of the manuscript.

- 698 The content is solely the responsibility of the authors and does not neces-
- 699 sarily represent the official views of the National Institutes of Health or the
- 700 National Science Foundation.

701

702

703 References

- 1. Bhatt S, Gething PW, Brady OJ, Messina JP, Farlow AW, Moyes CL, et al. The global distribution and burden of dengue. Nature. 2013;496(7446):504.
- Baud D, Gubler DJ, Schaub B, Lanteri MC, Musso D. An update on Zika virus infection.
- 708 The Lancet. 2017;390(10107):2099-109.
- 709 3. Petersen LR, Jamieson DJ, Powers AM, Honein MA. Zika Virus. New England Journal 710 of Medicine. 2016;374(16):1552-63.
- 711 4. Nasci RS. Movement of Chikungunya Virus into the Western Hemisphere. Emerging
- 712 Infectious Diseases. 2014;20(8):1394-5.
- 713 5. Nogueira RM, Eppinghaus AL. Dengue virus type 4 arrives in the state of Rio de Janeiro:
- 714 a challenge for epidemiological surveillance and control. Memórias do Instituto Oswaldo Cruz.
- 715 2011;106:255-6.
- 716 6. Zanluca C, de Melo VCA, Mosimann ALP, dos Santos GIV, dos Santos CND, Luz K.
- 717 First report of autochthonous transmission of Zika virus in Brazil. Memórias do Instituto
- 718 Oswaldo Cruz. 2015;110(4):569-72.
- 719 7. Nunes MRT, Faria NR, de Vasconcelos JM, Golding N, Kraemer MUG, de Oliveira LF,
- 720 et al. Emergence and potential for spread of Chikungunya virus in Brazil. BMC Medicine.
- 721 2015;13(1):102.
- Nogueira RMR, Miagostovich MP, Schatzmayr HG, Santos FBd, Araújo ESMd, Filippis
- 723 AMBd, et al. Dengue in the State of Rio de Janeiro, Brazil, 1986-1998. Memórias do Instituto
- 724 Oswaldo Cruz. 1999;94:297-304.
- 725 9. Nogueira RMR, Miagostovich MP, Lampe E, Souza RW, Zagne SMO, Schatzmayr HG.
- 726 Dengue Epidemic in the State of Rio de Janeiro, Brazil, 1990-1: Co-Circulation of Dengue 1 and
- 727 Dengue 2 Serotypes. Epidemiol Infect. 1993;111(1):163-70.
- 728 10. Miagostovich MP, Nogueira RM, Cavalcanti S, Marzochi KB, Schatzmayr HG. Dengue
- 729 epidemic in the state of Rio de Janeiro, Brazil: virological and epidemiological aspects. Revista
- 730 do Instituto de Medicina Tropical de São Paulo. 1993;35(2):149-54.
- 731 11. O'Reilly KM, Lowe R, Edmunds WJ, Mayaud P, Kucharski A, Eggo RM, et al.
- 732 Projecting the end of the Zika virus epidemic in Latin America: a modelling analysis. BMC
- 733 medicine. 2018;16(1):180-.
- 734 12. Struchiner CJ, Rocklöv J, Wilder-Smith A, Massad E. Increasing Dengue Incidence in
- 735 Singapore over the Past 40 Years: Population Growth, Climate and Mobility. PLOS ONE.
- 736 2015;10(8):e0136286.
- 737 13. Stewart-Ibarra AM, Lowe R. Climate and non-climate drivers of dengue epidemics in
- 738 southern coastal ecuador. Am J Trop Med Hyg. 2013;88(5):971-81.
- 739 14. Vincenti-Gonzalez MF, Tami A, Lizarazo EF, Grillet ME. ENSO-driven climate
- 740 variability promotes periodic major outbreaks of dengue in Venezuela. Scientific reports.
- 741 2018;8(1):5727-.

- 742 15. Hii YL, Rocklöv J, Ng N, Tang CS, Pang FY, Sauerborn R. Climate variability and
- 743 increase in intensity and magnitude of dengue incidence in Singapore. Global Health Action.
- 744 2009;2(1):2036.
- 745 16. Cazelles B, Chavez M, McMichael AJ, Hales S. Nonstationary Influence of El Niño on
- 746 the Synchronous Dengue Epidemics in Thailand. PLOS Medicine. 2005;2(4):e106.
- 747 17. Harris M, Caldwell JM, Mordecai EA. Climate drives spatial variation in Zika epidemics
- 748 in Latin America. Proceedings of the Royal Society B: Biological Sciences.
- 749 2019;286(1909):20191578.
- 750 18. Recker M, Blyuss Konstantin B, Simmons Cameron P, Hien Tran T, Wills B, Farrar J, et
- 751 al. Immunological serotype interactions and their effect on the epidemiological pattern of
- dengue. Proceedings of the Royal Society B: Biological Sciences. 2009;276(1667):2541-8.
- 753 19. Reich NG, Shrestha S, King AA, Rohani P, Lessler J, Kalayanarooj S, et al. Interactions
- 754 between serotypes of dengue highlight epidemiological impact of cross-immunity. Journal of
- 755 The Royal Society Interface. 2013;10(86).
- 756 20. Cummings DAT, Schwartz IB, Billings L, Shaw LB, Burke DS. Dynamic effects of
- 757 antibody-dependent enhancement on the fitness of viruses. Proceedings of the National Academy
- 758 of Sciences of the United States of America. 2005;102(42):15259.
- 759 21. Ferguson N, Anderson R, Gupta S. The effect of antibody-dependent enhancement on the
- 760 transmission dynamics and persistence of multiple-strain pathogens. Proceedings of the National
- Academy of Sciences of the United States of America. 1999;96(2):790-4.
- 762 22. Bjørnstad ON, Finkenstädt BF, Grenfell BT. Dynamics of measles epidemics: estimating
- 763 scaling of transmission rates using a time series SIR model. Ecological Monographs.
- 764 2002;72(2):169-84.
- 765 23. Earn DJD, Rohani P, Bolker BM, Grenfell BT. A Simple Model for Complex Dynamical
- 766 Transitions in Epidemics. Science. 2000;287(5453):667-70.
- 767 24. Finkenstädt B, Grenfell B. Empirical determinants of measles metapopulation dynamics
- 768 in England and Wales. Proc Biol Sci. 1998;265(1392):211-20.
- 769 25. Graham M, Winter AK, Ferrari M, Grenfell B, Moss WJ, Azman AS, et al. Measles and
- 770 the canonical path to elimination. Science. 2019;364(6440):584-7.
- 771 26. Grenfell BT, Bjørnstad ON, Finkenstädt BF. DYNAMICS OF MEASLES EPIDEMICS:
- 772 SCALING NOISE, DETERMINISM, AND PREDICTABILITY WITH THE TSIR MODEL.
- 773 Ecological Monographs. 2002;72(2):185-202.
- 774 27. Domenech de Cellès M, Magpantay FMG, King AA, Rohani P. The impact of past
- 775 vaccination coverage and immunity on pertussis resurgence. Science Translational Medicine.
- 776 2018;10(434):eaaj1748.
- 777 28. Lavine JS, King AA, Bjørnstad ON. Natural immune boosting in pertussis dynamics and
- 778 the potential for long-term vaccine failure. Proceedings of the National Academy of Sciences.
- 779 2011;108(17):7259-64.
- 780 29. Stone L, Olinky R, Huppert A. Seasonal dynamics of recurrent epidemics. Nature.
- 781 2007;446(7135):533.
- 782 30. Lowe R, Bailey TC, Stephenson DB, Jupp TE, Graham RJ, Barcellos C, et al. The
- 783 development of an early warning system for climate-sensitive disease risk with a focus on
- 784 dengue epidemics in Southeast Brazil. Statistics in medicine. 2012;32(5):864-83.
- 785 31. Ferguson NM, Cucunubá ZM, Dorigatti I, Nedjati-Gilani GL, Donnelly CA, Basáñez M-
- 786 G, et al. Countering the Zika epidemic in Latin America. Science. 2016;353(6297):353-4.
- 787 32. Imai N, Dorigatti I, Cauchemez S, Ferguson NM. Estimating Dengue Transmission
- 788 Intensity from Case-Notification Data from Multiple Countries. PLOS Neglected Tropical
- 789 Diseases. 2016;10(7):e0004833.

- 790 33. Figueiredo LTM, Cavalcante SMB, Simoes MC. Dengue serologic survey of
- 791 schoolchildren in Rio de Janeiro, Brazil, in 1986 and 1987. 1990.
- 792 34. Olinky R, Huppert A, Stone L. Seasonal dynamics and thresholds governing recurrent
- 793 epidemics. Journal of Mathematical Biology. 2008;56(6):827-39.
- 794 35. (IBGE) BIoGaS. Brazil Demographic Census 2010. . Rio de Janeiro, Brazil: Brazilian
- 795 Institute of Geography and Statistics (IBGE). 2012.
- 796 36. (IBGE) BIoGaS. "Censo Demographico- 1991-Rio de Janeiro". 1991; "Censo
- 797 demográfico : 1991 : resultados do universo relativos as características da população e dos
- 798 domicílios"(Table 1.4: "População residente, por grupos de idade, segundo ti lolesorregiàes, as
- 799 Microrregiões, os Municípios, os Distritos e o sexo"):32-41.
- 800 37. (IBGE) BIoGaS. Censo Demográfico. 2000(População residente, sexo e situação do
- 801 domicílio; Total column).
- 802 38. Dick OB, San Martín JL, Montoya RH, del Diego J, Zambrano B, Dayan GH. The
- 803 history of dengue outbreaks in the Americas. The American journal of tropical medicine and
- 804 hygiene. 2012;87(4):584-93.
- 805 39. Severo OP. Eradication of the Aedes aegypti mosquito from the Americas. 1955.
- 806 40. Löwy I. Leaking Containers: Success and Failure in Controlling the Mosquito Aedes
- 807 aegypti in Brazil. Am J Public Health. 2017;107(4):517-24.
- 808 41. PAHO. The feasibility of erradicating Aedes aegypti in the Americas. Pan Am J Public
- 809 Health. 1997;1.
- 810 42. Souza NCSe, Félix AC, de Paula AV, Levi JE, Pannuti CS, Romano CM. Evaluation of
- 811 serological cross-reactivity between yellow fever and other flaviviruses. International Journal of
- 812 Infectious Diseases. 2019;81:4-5.
- 813 43. de Carvalho JAM. Demographic dynamics in Brazil: recent trends and perspectives.
- 814 Brazilian journal of population studies. 1997;1(1):5-23.
- 815 44. Codeço CT, Villela DA, Coelho FC. Estimating the effective reproduction number of
- 816 dengue considering temperature-dependent generation intervals. Epidemics. 2018;25:101-11.
- 817 45. Coelho FC, Carvalho LMd. Estimating the Attack Ratio of Dengue Epidemics under
- 818 Time-varying Force of Infection using Aggregated Notification Data. Scientific Reports.
- 819 2015;5:18455.
- 820 46. Honório NA, Codeço CT, Alves FC, Magalhães MAFM, Lourenço-de-Oliveira R.
- 821 Temporal Distribution of Aedes aegypti in Different Districts of Rio De Janeiro, Brazil,
- Measured by Two Types of Traps. Journal of Medical Entomology. 2009;46(5):1001-14.
- 823 47. Mordecai EA, Cohen JM, Evans MV, Gudapati P, Johnson LR, Lippi CA, et al.
- 824 Detecting the impact of temperature on transmission of Zika, dengue, and chikungunya using
- 825 mechanistic models. PLOS Neglected Tropical Diseases. 2017;11(4):e0005568.
- 826 48. Otero M, Schweigmann N, Solari HG. A Stochastic Spatial Dynamical Model for Aedes
- 827 Aegypti. Bulletin of Mathematical Biology. 2008;70(5):1297.
- 828 49. Musa SS, Zhao S, Chan H-S, Jin Z, He D. A mathematical model to study the 2014–2015
- 829 large-scale dengue epidemics in Kaohsiung and Tainan cities in Taiwan, China. Mathematical
- 830 biosciences and engineering. 2019.
- 831 50. Imai N, Dorigatti I, Cauchemez S, Ferguson NM. Estimating dengue transmission
- 832 intensity from sero-prevalence surveys in multiple countries. PLoS neglected tropical diseases.
- 833 2015;9(4):e0003719-e.
- 834 51. Ap. 127 Die in Floods and Mud Slides in Brazil. New York Times. 1988 02/08/
- 835 1988 Feb 08.
- 836 52. Fouque F, Carinci R, Gaborit P, Issaly J, Bicout DJ, Sabatier P. Aedes aegypti survival
- and dengue transmission patterns in French Guiana. Journal of Vector Ecology. 2006;31(2):390-
- 838 400.

- 839 53. Benedum CM, Seidahmed OME, Eltahir EAB, Markuzon N. Statistical modeling of the
- 840 effect of rainfall flushing on dengue transmission in Singapore. PLOS Neglected Tropical
- 841 Diseases. 2018;12(12):e0006935.
- 842 54. Seidahmed OME, Eltahir EAB. A Sequence of Flushing and Drying of Breeding Habitats
- 843 of Aedes aegypti (L.) Prior to the Low Dengue Season in Singapore. PLOS Neglected Tropical
- 844 Diseases. 2016;10(7):e0004842.
- 845 55. Kakarla SG, Caminade C, Mutheneni SR, Morse AP, Upadhyayula SM, Kadiri MR, et al.
- 846 Lag effect of climatic variables on dengue burden in India. Epidemiol Infect. 2019;147:e170.
- 847 56. Katzelnick LC, Fonville JM, Gromowski GD, Arriaga JB, Green A, James SL, et al.
- 848 Dengue viruses cluster antigenically but not as discrete serotypes. Science.
- 849 2015;349(6254):1338.
- 850 57. Bell SM, Katzelnick L, Bedford T. Dengue genetic divergence generates within-serotype
- antigenic variation, but serotypes dominate evolutionary dynamics. eLife. 2019;8:e42496.
- 852 58. Romeo-Aznar V, Paul R, Telle O, Pascual M. Mosquito-borne transmission in urban
- 853 landscapes: the missing link between vector abundance and human density. Proceedings of the
- 854 Royal Society B: Biological Sciences. 2018;285(1884):20180826.
- 855 59. Stoddard ST, Forshey BM, Morrison AC, Paz-Soldan VA, Vazquez-Prokopec GM,
- 856 Astete H, et al. House-to-house human movement drives dengue virus transmission. Proceedings
- 857 of the National Academy of Sciences. 2013;110(3):994-9.
- 858 60. Guzzetta G, Marques-Toledo CA, Rosà R, Teixeira M, Merler S. Quantifying the spatial
- 859 spread of dengue in a non-endemic Brazilian metropolis via transmission chain reconstruction.
- 860 Nature Communications. 2018;9(1):2837.
- 861 61. Organization WH. Dengue and severe dengue. Fact sheet Updated April 2017. 2017.
- 862 62. Organization WH. Dengue and severe dengue. World Health Organization. Regional
- 863 Office for the Eastern Mediterranean; 2014.
- 864 63. Bretó C, Ionides EL. Compound markov counting processes and their applications to
- 865 modeling infinitesimally over-dispersed systems. Stochastic Processes and their Applications.
- 866 2011;121(11):2571-91.
- 867 64. He D, Ionides EL, King AA. Plug-and-play inference for disease dynamics: measles in
- 868 large and small populations as a case study. Journal of the Royal Society Interface.
- 869 2009;7(43):271-83.

- 870 65. Ionides EL, Nguyen D, Atchadé Y, Stoev S, King AA. Inference for dynamic and latent
- 871 variable models via iterated, perturbed Bayes maps. Proceedings of the National Academy of
- 872 Sciences. 2015;112(3):719-24.